Princeton/$\mu\mu$/99-15
S.E. Vahsen, C. Lu, K.T. McDonald,
February 1999

Precision Timing via Čerenkov Radiation, II[1]

Abstract

With an eye to the proposed muon-cooling experiment [1], we have investigated the performance of a charged particle timing device using ultrafast photomultipliers (PMT's) to view Čerenkov radiation from quartz-bars. We have performed a simulation which indicates that the rms timing, σ_t, of 165-MeV/c muons could be determined over a beam of 10-cm radius to 10 ps via Čerenkov radiation emitted in 1×1 cm^2 quartz bars viewed by Hamamatsu R3809U microchannel-plate photomultipliers (MCP-PMT's). This result assumes that the arrival time of individual photons can be measured by the MCP-PMT's with an accuracy of 11 ps (rms), as claimed by the manufacturer. We have performed measurements of the transit-time spread in these photomultipliers and of the time jitter in the detection electronics, which are the parameters that determine the singlephoton time resolution. We conclude that the large variation in the amplitude of the PMT's output-signal results in time-shifts in the discriminator, which makes 10-ps timing difficult at high efficiencies. These results suggest we move on to investigate the performance of a system that uses pulse-height information to correct for time walk (the dependence of time assigned to a pulse on the pulse's amplitude). We have performed a Monte Carlo simulation which indicates that this technique may allow us to approach the desired timing performance at high efficiencies.

1 Introduction

1.1 Timing in the Muon-Cooling Experiment

One of the most critical problems associated with a potential future muon collider is the cooling of the muon beam. In the hope of demonstrating the feasibility of ionization cooling as a solution to this problem, the Muon Collider Collaboration is working towards a muon-cooling demonstration experiment [1]. Even though not all aspects of this experiment have been finalized, the basic scheme involves passing single muons through a cooling apparatus, and characterizing their 6 phase-space parameters before and after the cooling. A bunch of muons can then be formed in software at a later time, so that the effects of the cooling apparatus on the phase space of a complete bunch can be determined. This scheme is thought to account for all effects except space charge.

One of the most critical measurements that is required on the muons is their time of arrival at the entrance and exit of the cooling channel. It has been proposed to carry

[1] An earlier version of this report has been submitted at Princeton University by Sven Vahsen in order to meet the experimental project requirement of the Physics Department's General Examination.

out this measurement with an elaborate instrumentation scheme which would enable time measurements with a standard deviation $\sigma_t \approx 8$ ps [2]. During the development of this instrumentation scheme, Alan Bross [3] raised the question whether time resolution on the order of 8 ps could be achieved by an alternative (and less costly) method - timing with ultrafast PMT's viewing Čerenkov radiation from quartz bars. It has been the purpose of this work to estimate the timing performance of such an alternative method.

1.2 Timing via Čerenkov Radiation

Even though the emission of Čerenkov radiation due to a charged particle traversing an optically dense material is a very fast process, on the time-scale of femto seconds, using this Čerenkov radiation to obtain pico second estimates of the arrival time of the charge particle is a tricky business. This is because the time resolution one can obtain in practice is limited by both the spatial distribution of the emitted photons, and by the process used to convert these photons into a useful electrical signal.

The number of visible Čerenkov photons emitted by a charged particle traversing a material at a velocity $v \approx c$ is on the order of 500/cm [4]. In order to get enough photons (after losses due to collection and detector efficiencies) to result in a useful signal, we typically need the charged particle to traverse a few cm of material. However, 10 ps corresponds to 3 mm at the speed of light, so that the distribution of photons along the charged particle trajectory results in time jitter much larger than the intrinsic time-scale of the Čerenkov process. In addition, the photons typically need to propagate to a device where they are converted into an electrical signal, and if they happen to take paths that differ in length by more than a few mm, we again get time-jitter in the 10-ps range. Of course, the collective information of all the photons from a given event (due to one charged particle traversing the detector) results in an improvement of the time-information in that the arrival time of the individual photons can be averaged to estimate the arrival time of the charged particle with a standard deviation less than that of individual photons.

The conversion of photons into an electrical signal is usually achieved via the photoelectric effect. The incident photons give energy to valence electrons of a photocathode, resulting in some of these electrons being emitted as photoelectrons. The ratio of incident photons to emitted electrons is referred to as the quantum efficiency of the photocathode, η, with typical values around 25% for visible light. The number of photoelectrons arising from the Čerenkov radiation of one charged particle is in most cases far too low to yield a useful electrical signal (see section 2), so that some sort of amplification is needed. In conventional photo-multipliers, this is achieved by accelerating the photoelectrons to kinetic energies of a few hundred eV, which is large enough to knock out multiple electrons from a dynode. This process of acceleration and multiplication by secondary emission is referred to as one stage of the photomultiplier, and by employing multiple stages one can achieve an exponential growth in the number of electrons. After the last stage of the photomultiplier, the resulting electrons (typically on the order of 10^5) are focused onto the phototube anode, and result in the electrical output signal.

The time it takes from when a photoelectron is emitted at the cathode until the resulting electron avalanche has produced the peak output signal at the anode is referred to as the photomultiplier's transit time. The interesting quantity for timing purposes is not the transit

time itself, but it's variation from event to event, referred to as the transit-time jitter or transit-time spread, usually stated in terms of the full width at half maximum (FWHM) or by the standard deviation, σ_t, of the transit-time distribution. Since the electrons in the photomultiplier propagate at a velocity much less than the speed of light (e.g. $E_{\rm k} = 200$ eV is equivalent to $\beta = v/c \approx 0.03$), tiny variations in the path taken by the electrons result in relatively large transit-time jitter. For instance, a time spread of 10 ps at $\beta = 0.03$ corresponds to a distance variation of only 90 μm.

In microchannel-plate photomultipliers (MCP-PMT's), the electrons are multiplied in micron-sized channels of total length about 1mm. This confinement of the possible electron-path limits the possible variation in transit time, resulting in the amazing timing performance of these devices. For instance, Hamamatsu reports the transit-time spread of their R3809U MCP-PMT (6 μm channels) to be better than $\sigma_{\rm t} = 11$ ps.

2 Simulation of Timing via Čerenkov Radiation

In order to estimate the timing performance of a device based on ultrafast PMT's viewing Čerenkov radiation from quartz-bars, we started out simulating the corresponding scenario. In order to limit this report to a reasonable size, we only quote a few numerical results of the simulation, and refer to our previous report [4] as an appendix. In particular, see section 5 and fig. 8 of that report for a discussion and sketch of the proposed timing-device.

The simulation indicates that a timing device for 165-MeV/c muons based on Hamamatsu R3809U MCP-PMT's viewing Čerenkov radiation from 1×1 cm quartz bars could detect an average of about 60 photons per muon (that number includes absorption and reflection losses in the quartz bar as well as the quantum-efficiency of the PMT's photocathode). By combining the *exact* arrival time of all the photons, one could in principle estimate the muon's arrival time with an accuracy of $\sigma_t \approx 5$ ps, which is the intrinsic time resolution of the device. However, our ability to measure the arrival time of individual photons is limited by the transit-time spread of the MCP-PMT, as well as time jitter in the necessary detection electronics. Our estimate of the time resolution that can be obtained in practice (including a single photon time resolution of $\sigma = 11$ ps, as reported by Hamamatsu for the R3809U MCP-PMT [5]) is thus somewhat larger, on the order of $\sigma_t \approx 9 - 10$ ps. This is very close to the time resolution needed for the muon-cooling experiment. Since the exact value predicted for σ_t depends on the single photon time resolution, we have carried out our own measurements, which we report on below.

3 Measurement of Single Photon Time Resolution

3.1 Introduction

Hamamatsu reports that the transit-time spread of the R3809U MCP-PMT has been measured to $\sigma_{\rm PMT} = 10.8$ ps [5], *including* time jitter of all electronics. Other recent experiments however [6, 7, 8], indicate that $\sigma_{\rm PMT}$ may be somewhat higher. These measurements typically involve estimating the PMT timing performance from the overall timing performance of the system. For instance, the actual time-jitter measured by Hamamatsu for our MCP-PMT

(s/n ct100) using a picosecond light pulser was FWHM = 42 ps, from which they subtracted the estimated jitter of the pulser, FWHM = 35 ps, in quadrature, to arrive at FWHM = 23 ps, or $\sigma_{\mathrm{PMT}} = 9.9$ ps.

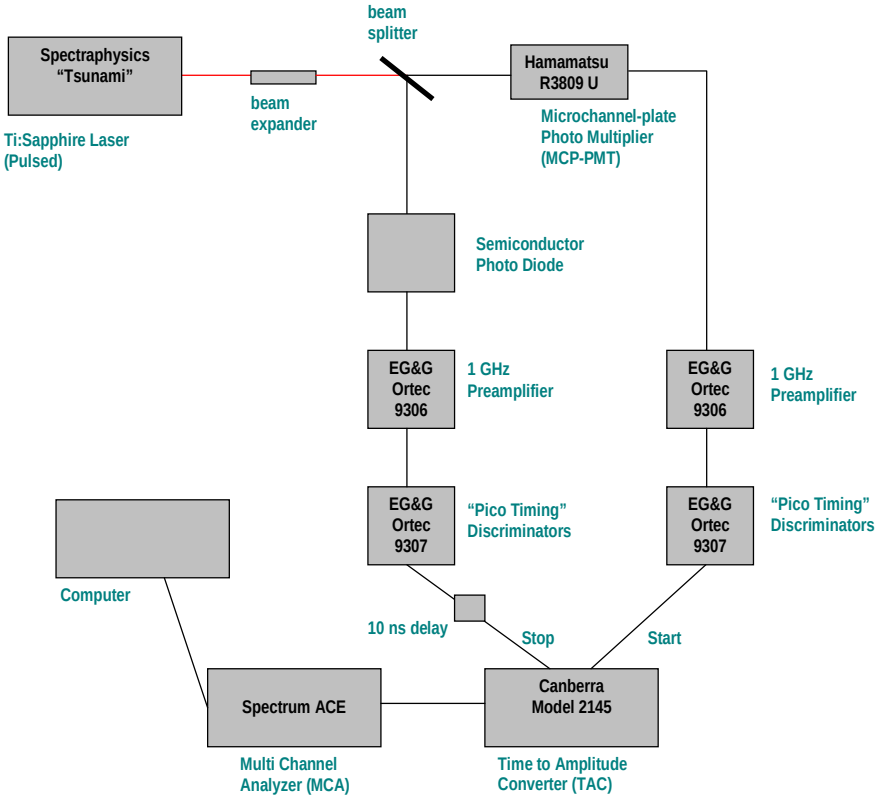

Figure 1: Setup used to measure transit time spread of Hamamatsu R3809U Microchannel Plate Photomultiplier (MCP-PMT).

We used the setup of fig. 1 to measure the transit-time distribution of the Hamamatsu R3809U MCP-PMT. The Ti:Sapphire laser emits light pulses shorter than 1 ps, at a rate of 71.4 MHz. Pulses propagate through the beam expander to the beam splitter, from where some of the photons will propagate to a reference photo diode (see section 3.2), some to the PMT. We typically want as many photons as possible to hit the diode, while we usually want 0 or 1 photon from each pulse to hit the PMT (see section 3.6). The beam incident on the PMT is attenuated with neutral-density filters to achieve the desired rate of incident photons. The outputs of both photo devices are fed into EG&G Ortec 9306 1-GHz preamplifiers, which smear out the signals somewhat. (PMT-signal rise time $\approx$ 150 ps, diode signal rise time $\approx$ 80 ps). The preamps feed into EG&G Ortec 9307 "pico-TIMING" discriminators (see section 3.3 for performance specifications). The (fast NIM) logic signal outputs from the discriminators are used as start and stop signal for a Canberra Model 2145 time to amplitude converter (TAC). The TAC requires a time difference $t > 11.8$ ns between the start and the stop signal, which we achieve by delaying the stop signal. A personal computer with an EG&G Spectrum ACE 8000-channel multichannel analyzer card

(MCA) records the pulse-height distribution from the TAC output. With the MCA properly calibrated, this gives us the distribution of time differences between the PMT and photodiode signals arising from the same laser pulse. Each time difference measured will include not only the transit time of the PMT, but also the time jitter due to the diode, discriminators, the preamps, the TAC, the MCA, cables and connectors. Some of these effects depend on the signal amplitude, so that the stability of the laser intensity affects the time resolution as well. Since the time difference measured for each laser pulse can be regarded as the sum of the signal transit time of each system component, the time distribution measured will be the convolution of the PMT transit-time distribution with the time distribution due to other system components.

To properly interpret our measurement of the PMT transit-time spread, we therefore need accurate information on the timing performance of the other system components shown in fig. 1. (This information is of course also valuable in itself, since many of these components will necessarily be part of any complete timing device.) To this end, we have tested all the system components systematically for their timing performance. The details of these tests will be reported in the next sections. The dominant sources of time jitter, apart from the transit-time spread of the PMT, were found to be the time distribution of the diode signal (see section 3.2) and the variation in discriminator timing due to the large variations in the PMT-signal amplitude (see section 3.3). The time jitter of the other system components combined was measured to be $\sigma_t \approx$ 4-5 ps at constant pulse amplitude.

3.2 Time Reference - Semiconductor Photodiode

An Epitaxx ETC 60B InGaAs 4-GHz photodiode served as the time reference in the measurement of the MCP-PMT transit-time spread, as shown in fig. 1.

To get information on the diode's timing-performance, we used the setup of fig. 2. The start signal feeding into the TAC is delayed by about 18 ns (10 ns delay + 1.5 m of 50Ω SMA-cable) relative to the stop signal. Since the laser-pulse separation at 71.4 MHz is about 14 ns, this ensures that the diode signals from two different laser pulses give rise to the start and stop signals. The time difference measured therefore includes the pulse-to-pulse time jitter of the laser, as well as the time jitter of the diode start and stop signals. The time distribution measured (see fig. 3) has a standard-deviation of $\sigma_t = 12.0$ ps (FHWM = 28 ps), which tells us that the time jitter of each diode signal (start and stop), σ_{td}, is less than 12.0 ps $/\sqrt{2} = 8.5$ ps.

During the measurement of the diode-signal's time jitter, we encountered some instability problems which have not been resolved completely. Typically, the mean of the time distribution, such at that shown in fig. 3, drifted with time, and after about 30 minutes of operation the peak would split into two peaks separated by about 40 ps. When observed on a Tektronix 7104 1-GHz oscilloscope, the amplified diode signal showed an amplitude-oscillation of about 40 mV peak-to-peak (for a 900-mV signal). This amplitude oscillation can be related to a time oscillation via the discriminator time walk (see section 3.3). The slope of the time-walk plot (fig. 5) at 900 mV indicates that an amplitude variation of 40 mV would result in time-jitter of perhaps ± 5ps, which is not large enough to explain the observed double-peak. However, the manufacturer of the discriminator reports that for signals with rise times less than 350 ps, the effective discriminator threshold will be higher than

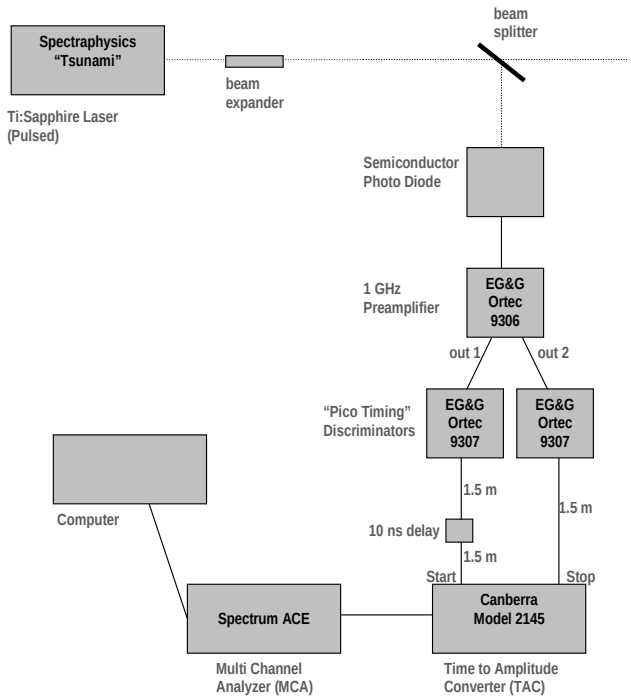

Figure 2: Setup used to determine time jitter of the semiconductor photodiode signal that was used as a time reference.

selected, due to the limited time response of the discriminator's comparator circuits. It is therefore possible that the fast diode signal (80-ps rise) will result in time walk equivalent to a slower signal (as used to measure the discriminator time-walk) of lower amplitude. This could explain the 40-ps jitter observed, because we did observe double-peaks in the time-spectrum of the discriminator even for constant amplitude signals for amplitudes below 150 mV (see section 3.3). This issue has not been completely resolved.

The observed amplitude variation seems to arise from two effects, an oscillation in the laser intensity at a frequency of about 60 Hz, as well as an oscillation in the laser-beam position which would move the beam partially off the diode's sensitive area. Since the time-walk of the discriminators is smaller for signal amplitudes above 1.5 V (see fig. 5), the effect of the amplitude oscillation can be reduced by keeping the signal amplitude large. To achieve large signal amplitudes, we had to place the diode at a position along the beam where the beam's radius is a minimum and the beam thus more intense. However, the smaller beam radius makes the setup more vulnerable to the second effect (oscillation in the laser beam position). It was thus a tricky issue to adjust the diode's position in the beam in order to achieve the best possible trade-off between the two effects.

The laser beam position also has a slow drift on the time-scale of hours. By changing the laser-cavity mirrors' position slightly, one could often reposition the beam to achieve a fairly stable signal, but on a timescale of 1/2 hour the beam would again drift to an unstable position.

We circumvented these stability problems by adjusting the beam so that the diode-signal

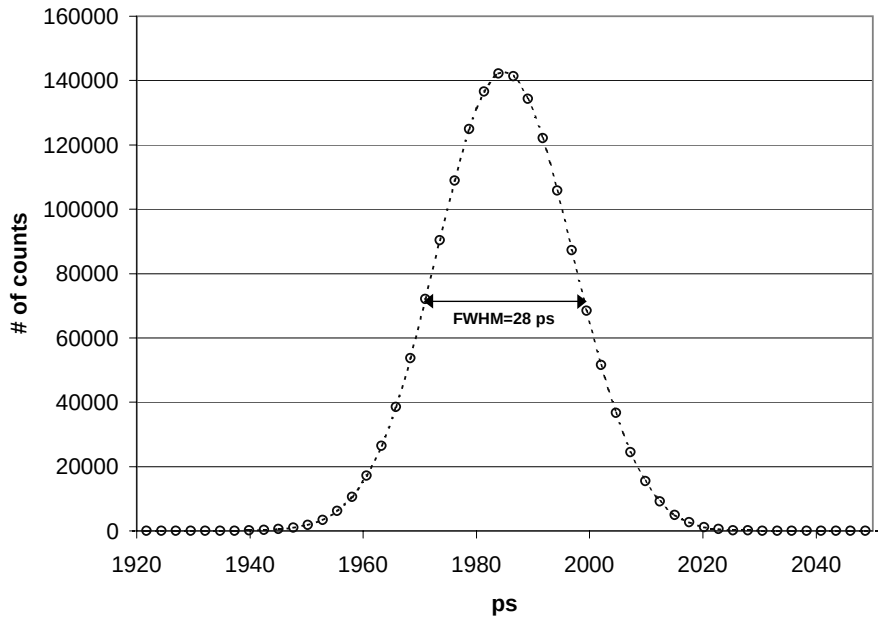

Figure 3: Time distribution obtained by using the semiconductor photodiode output from two different laser pulses as start and stop signal. Since this includes time jitter from all electronics, we conclude that the diode signal jitter, $\sigma_{\rm td} < \frac{28.15ps}{2.35\sqrt{2}} \approx 8.5$ ps.

was stable, performing the necessary measurements within 1/2 hour, and then re-measuring the diode signal afterwards. The diode signal time spread was usually found to have increased somewhat during this time, so that the exact diode time jitter that has to be deconvoluted from the PMT transit-time spread was estimated as the mean of the initial and final values. The distribution of fig. 3 with $\sigma_{\rm td} = 8.5$ ps was measured following the PMT transit-time measurements reported in section 3.5. The diode time-distribution observed before the PMT measurements appeared somewhat unstable, with the standard deviation varying from $\sigma_{\rm td} = 6.7$ to 8.8 ps.

3.3 Discriminator Time Walk

The EG&G Ortec 9307 "pico-TIMING" discriminator is reported by the manufacturer to have ± 20 ps shift in output timing for signal amplitudes from -150mV to -1.5V, and typically ± 50 ps for signal amplitudes from -50mV to -5V (for 1-ns-wide pulses with 350-ps rise and fall times), which is better than the performance of constant-fraction discriminators for such fast signals. The timing is reported to have a temperature sensitivity $< \pm 10$ ps/°C. The discriminator has an adjustment labeled "slewing compensation", the setting of which can be determined by measuring the voltage of a test point. This adjustment allows the discriminator time walk to be optimized for a given pulseshape.

We used the setup of fig. 4 to measure the timing of the EG&G Ortec 9307 with varying pulse amplitude ("time walk"), using 1-ns-wide (minimum for the Lecroy 9212 pulser used)

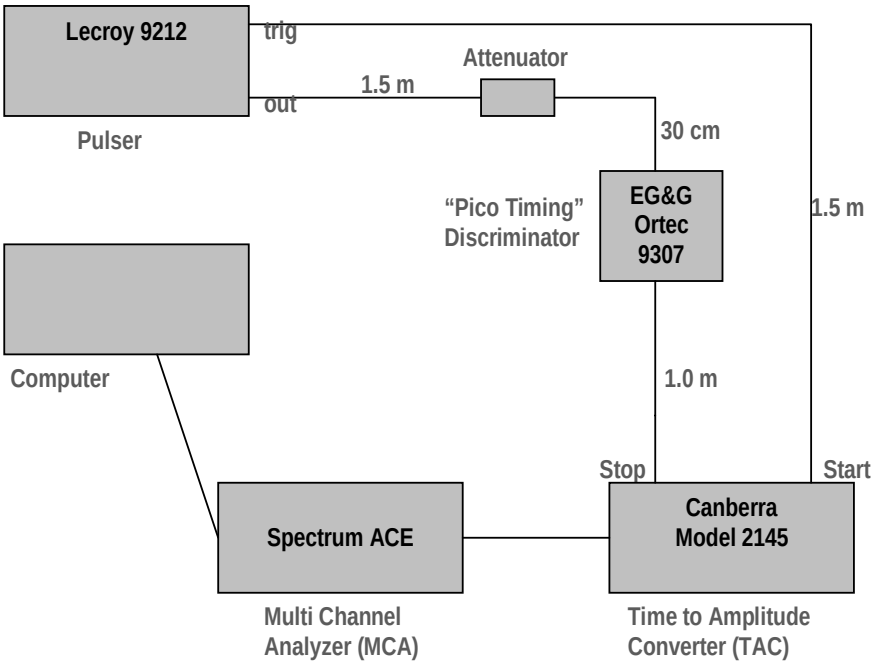

Figure 4: Setup used to measure time walk of EG&G Ortec 9307 discriminators.

pulses with 250-ps rise and fall times.

During initial measurements, we realized that changing the signal amplitude setting on the pulser affected the timing of the pulse output relative to the trigger output of the pulser. We therefore kept the pulser amplitude constant, and achieved varying pulse heights using an attenuator with variable attenuation. However, we also observed that the length difference in signal path taken for different attenuation settings inside the attenuator was enough to affect the timing on the timescale of interest. We therefore used a 20-GHz Tektronix Communication Signal Analyzer (CSA 803) to measure the signal delay in the attenuator for different attenuation settings. The attenuator delays were subtracted out from the total delays measured with the setup of fig. 4. The final result for one of the two discriminators is shown in fig. 5. The relative time reported corresponds to the peaks of the time-distributions measured. The width of the distribution (not shown) was typically σ = 6-8 ps, except for pulse amplitudes below 150 mV, where the time-spectrum would often become asymmetrical or split into two peaks separated by about 40 ps. These results are within the performance specifications of the manufacturer. The behavior for low amplitude pulses may explain the instability of the semiconductor diode's time spectrum, as discussed in section 3.2. The second discriminator showed very similar timing characteristics, with minor differences in the effect of the slewing compensation adjustment.

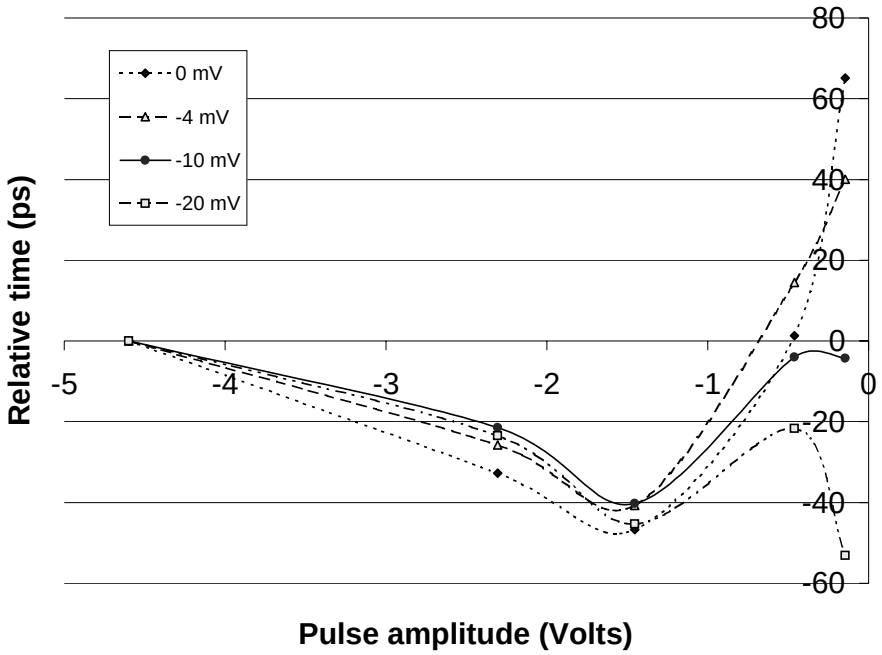

Figure 5: Time walk of EG&G Ortec 9307 "Pico Timing" discriminator for "slewing compensation" settings ranging from 0 mV to −20 mV. The relative time reported corresponds to the peaks of the time-distributions measured. The width of the distributions was typically σ = 6-8 ps, except for pulse amplitudes below 150 mV, where the time-spectrum would often become asymmetrical or split into two peaks separated by about 40 ps.

3.4 Hamamatsu R3809U Pulse-Height Distribution

In order to estimate the contribution of time walk to the overall time jitter of the system, we need information on the pulseheight distribution of the PMT's output-signal, which we measured with the setup of fig. 6. The EG&G Ortec 142 PC charge-sensitive preamplifier integrates the output of the MCP-PMT to give a slowly decaying output (exponential return to baseline in about 75 μs) with amplitude proportional to the total charge. The EG&G Ortec 570 Spectroscopy amplifier then reduces the width of this slow pulse to $\approx$ 1 μs, which meets the MCA input requirements. The HeNe laser-beam was attenuated until the discriminator trigger rate was less than 3000 Hz. This means that within the integration time of the pulse, $\approx$ 1 μs, we had an average of $3000 \times 10^{-6} = 0.003$ photons, which is low enough to ensure that we were observing mostly singlephoton pulses. (See section 3.6 for more details on this issue.)

We calibrated the MCA by using the "test" input of the charge-sensitive preamplifier. This input has a 1-pF capacitor, which allows the generation of a known amount of charge by applying a known voltage step with a signal generator. The calibration thus enables us to report the PMT's output-signal in terms of charge or number of electrons. Since we have made sure that the PMT pulses are largely singlephoton events (see section 3.6), the number of electrons in the output-signal is therefore equal to the single-photoelectron gain of the

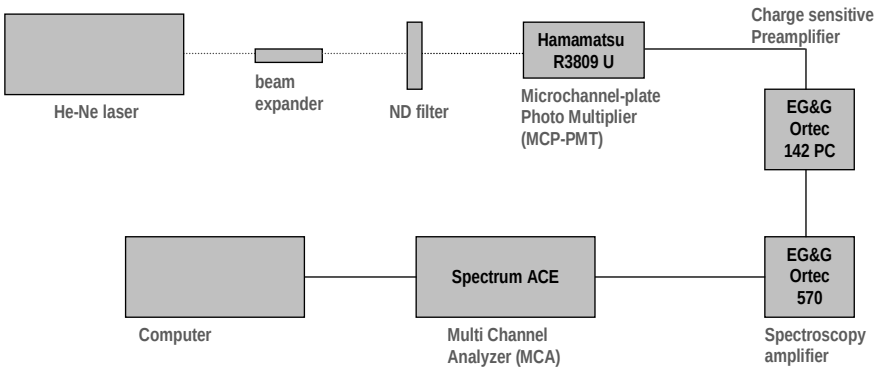

Figure 6: Setup used to measure Hamamatsu R3809U MCP-PMT pulse-height distributions.

PMT.

Fig. 7 shows pulseheight distributions measured for the R3809U MCP-PMT (s/n ct100). The distributions have mean gains $\mathrm{G_{PMT}}$ around 5.0×10^5 and 2.1×10^5 electrons per photoelectron for voltages of 3400 and 3200, respectively, while Hamamatsu reports the current gain of this specific MCP-PMT to be 1.4×10^6 and 6.4×10^5 for the same high-voltages. It thus appears that since these tubes were last tested by Hamamatsu in 1994, the gain of the PMT's has dropped by a factor of 3.

In order to get an appreciation of how this pulseheight distribution translates into time jitter due to discriminator time walk, we would like to know the output-signal amplitude of the preamp (following the MCP-PMT in the setup of fig. 1) for a given amount of total charge in the PMT pulse. We can estimate the preamp's mean peak output voltage as follows: Assuming an approximate triangular, amplitude-independent pulse shape with rise time t_r and fall time t_f, the total charge delivered by the PMT will be related to the peak output current by $Q = I_{\mathrm{peak}} \times (t_r + t_f)/2$. Thus, the peak voltage at the output of the preamp will be approximately

$$V_{\mathrm{peak}} = G_{\mathrm{preamp}} \times I_{\mathrm{peak}} \times Z_{\mathrm{in}} = G_{\mathrm{preamp}} \times \frac{2}{t_r + t_f} Q \times Z_{\mathrm{in}}, \tag{1}$$

where G_{preamp} and Z_{in} are the voltage gain and input impedance of the preamp.

We measured the preamp gain G_{preamp} to be 70 (we have altered the preamps slightly), the input impedance Z_{in} is 50 Ω, and using $t_r = 200$ ps and $t_f = 300$ ps (triangular fit to pulseshape reported by Hamamatsu) we obtain

$$V_{\mathrm{peak}} = 1.4 \times 10^{13} \times Q = 2.24 \times 10^{-6} \times \mathrm{G_{PMT}}, \tag{2}$$

where we used that $Q = \mathrm{G_{PMT}} \times \mathrm{e}$, where e is the electron charge in Coulombs. We can apply (2) to the measured single-photoelectron gain distributions. For instance, we learn that the preamp peak output voltage fed into the discriminator of the PMT-channel in the setup of fig. 1 will have a distribution with mean of approximately 1.1 V and 470 mV for PMT voltages of 3400 and 3200 Volts, respectively.

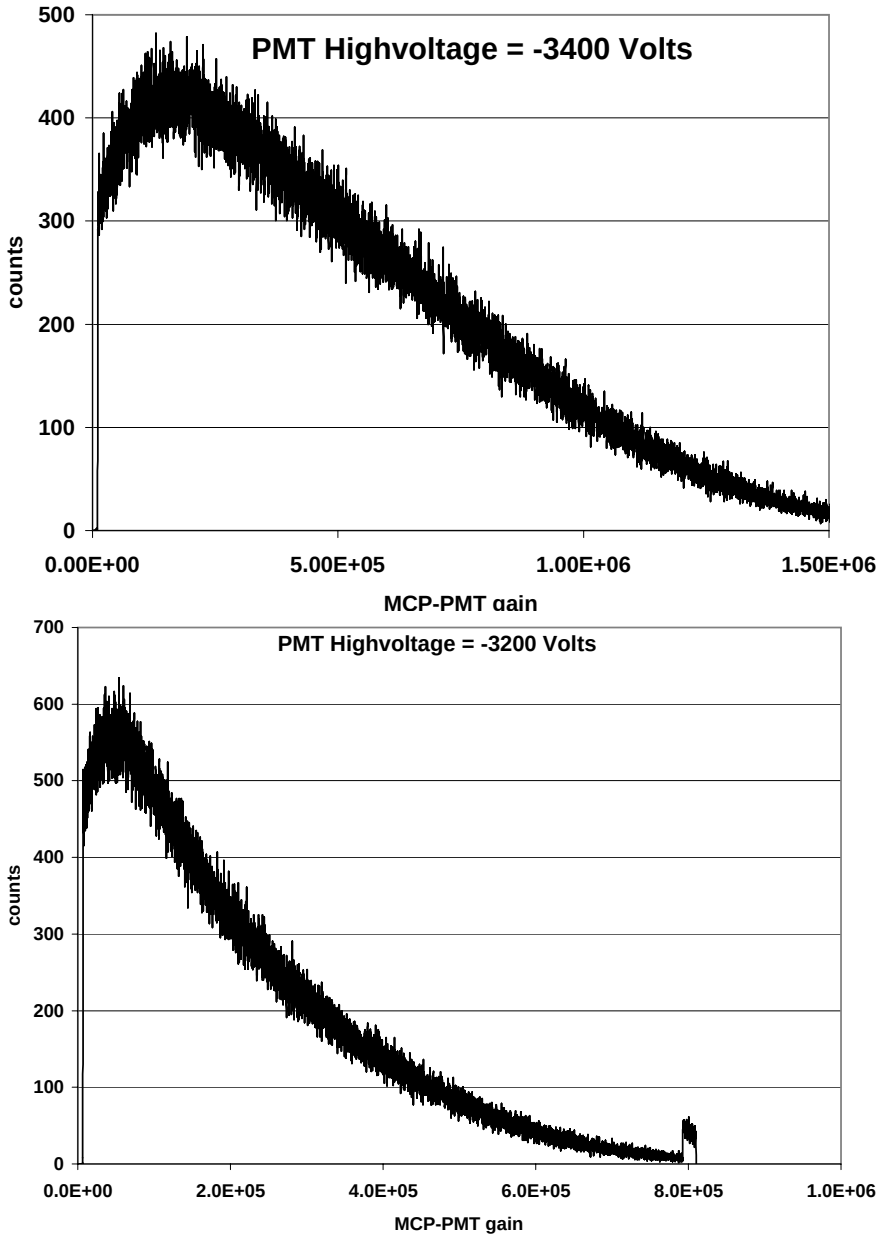

Figure 7: Single-photoelectron gain distributions for Hamamatsu R3809U MCP-PMT, at 3200 V (lower) and 3400 V (upper).

3.5 Hamamatsu R3809U Transit-Time Spread

Using the setup of fig. 1, we measured the transit-time spread of the Hamamatsu R3809U MCP-PMT, s/n ct100, for voltages of 3000 through 3400 Volts. The discriminator threshold was set to -25 mV (minimum), and the discriminator slewing compensation to -10 mV. The laser beam incident on the PMT was attenuated with neutral density filters so that the rate of incident photons was less than 73000 per second to ensure single photon events

(see section 3.6). Since there is a dead time on the order of microseconds associated with the TAC processing an event, we maximized our coincidence efficiency by using the PMT signal as start and the diode signal as stop. Each measurement was taken over a period of 60 seconds, and repeated twice for each PMT voltage. Due to the instability of the time reference discussed in section 3.2, the measurements had to be carried out quickly. The results are given in table 1.

Table 1: Results of transit-time distribution measurement for Hamamatsu R3809U MCP-PMT, s/n ct100, using the setup of fig. 1. $\mathrm{FWHM}_{\mathrm{total}}$ and σ_{total} include the time jitter of the time reference and all electronics. Subtracting the estimated jitter of the time reference, $\sigma_{\mathrm{td}} = 8.5$ ps, in quadrature gives $\sigma\prime_{\mathrm{PMT}}$, which includes jitter due to the PMT as well as the discriminator (see section 4).

PMT high-voltage (V)	$\mathrm{FWHM}_{\mathrm{total}}$ (ps)	σ_{total} (ps)	$\sigma\prime_{\mathrm{PMT}}$ (ps)
3000	46.96	19.98	18.0
3000	45.22	19.24	17.3
3100	42.01	17.88	15.7
3100	42.17	17.94	15.8
3200	44.31	18.86	16.8
3200	44.70	19.02	17.0
3300	54.50	23.19	21.6
3300	54.70	23.28	21.7
3400	56.41	24.00	22.4
3400	56.38	23.99	22.4

The data show that the drift of the system as a whole was such that the change in time resolution between the two measurements at constant voltage is less than 1% within 1 minute. The lowest time jitter measured was $\sigma\prime_{\mathrm{PMT}} \approx 16$ ps, for a voltage of 3100 V, and the corresponding time distribution is given in fig. 8. The prime in $\sigma\prime_{\mathrm{PMT}}$ indicates that this time jitter is not to solely due to the PMT, but that it also includes discriminator jitter. Section 4 reports on an attempt to estimate the magnitude of the discriminator's contribution to $\sigma\prime_{\mathrm{PMT}}$.

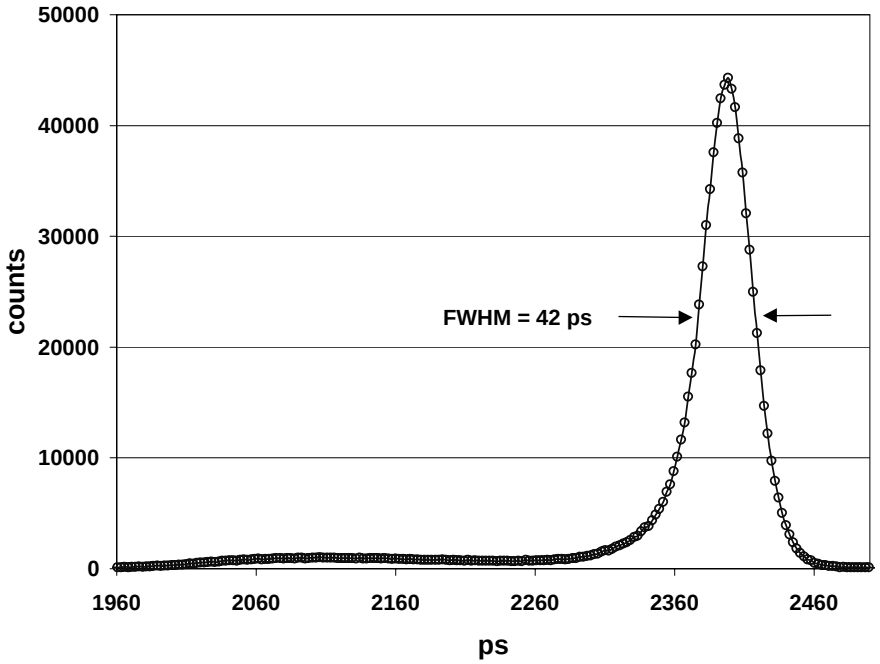

Figure 8: Transit-time distribution for Hamamatsu R3809U MCP-PMT (serial no. ct100), at 3100 V. The distribution includes time jitter of diode used as time reference ($\sigma_t \approx 8.5$ ps) and that of a EG&G Ortec 9307 discriminator. $\sigma'_{PMT} < \sqrt{(17.9)^2 - (8.5)^2}$ ps ≈ 16 ps.

3.6 Are We Really Doing *Single*photon Timing?

In interpreting our results, it is important to verify that the PMT is seeing singlephoton pulses, since we would expect improved timing for multiphoton pulses, which would lead us to overenthusiastic conclusions about the system's timing performance.

By feeding the discriminator output into a counter, we can compare the PMT pulserate to the laser's pulse-frequency of 71.4 MHz. If the average number of photons seen by the PMT per laser pulse is $\lambda \ll 1$, the number of photons per pulse will be Poisson-distributed with mean λ. The highest PMT pulserate used in the transit-time measurement was 73000 counts/second, or $\lambda = 1.02 \times 10^{-3}$. The probability of seeing one photon per pulse will then be $\lambda e^{-\lambda} \approx \lambda$, while the probability of seeing two photons per pulse will be $\lambda^2 e^{-\lambda}/2 \approx \lambda^2/2$. Therefore only approximately $\lambda/2 \approx 0.05\%$ of our events were two-photon events.

However, this assumes that we are certain that a typical PMT pulse due to a singlephoton event had an amplitude large enough to trigger the discriminator. Otherwise, we may have been observing only the few multiphoton pulses that make it past the discriminator. This was ruled out by observing PMT dark-current pulses, which will have amplitudes similar to those of singlephoton pulses. By making sure the dark-current pulses would trigger the discriminator, we were also ensuring that the singlephoton pulses would have amplitudes large enough to trigger the discriminator.

4 Monte Carlo Simulation of Discriminator Timimg

Since the time distributions obtained in the PMT transit-time measurement (such as in fig. 8) include time jitter due to the discriminator of the PMT channel, we would like to estimate the time distribution of the discriminator output pulses. This will allow us to give a better estimate of the PMT's timing performance, as well as an estimate of the timing performance one could hope to reach in a timing system that incorporates time walk correction. Such a system would record and store the amplitude as well as the arrival time of each pulse, and use this information to correct for discriminator time walk in software.

We estimate the time distribution of the discriminator output pulses with a Monte Carlo simulation. The simulation generates a total of 5000 PMT pulses. For each pulse, the PMT peak output amplitude is drawn from the probability distribution obtained by appropriately normalizing the singlephoton-gain distributions in fig. 7. The corresponding peak voltage at the preamp output is calculated using (2). This is the peak amplitude that the discriminator will "see". The discriminator's response time will have a distribution which depends on this amplitude. (The dependence of the mean of this distribution on the pulse amplitude is what results in a time walk plot such as fig. 5). The simulation looks up the mean and standard deviation of the time distribution corresponding to the discriminator input pulse amplitude, and generates a random time from a normal distribution with this mean and standard deviation. The resultant time is stored.

4.1 Estimate of PMT Transit-Time Spread

After repeating this procedure for 5000 pulses, we obtain an estimated distribution of discriminator output-pulse timing corresponding to the specified PMT singlephoton-gain distribution, which in turn depends on the PMT voltage. For instance, for a PMT voltage of 3400 V, we predict a discriminator time distribution with standard deviation, $\sigma_{\rm disc}$, of 13.5 to 14.1 ps (see fig.9). We state our prediction as a range, because we simulated two different scenarios, reflecting the somewhat unpredictable behavior of the discriminator time distribution for pulses with amplitude less than 150 mV. For a PMT voltage of 3200 V we predict $\sigma_{\rm disc}$ between 10.8 and 13.6 ps. We subtract these numbers in quadrature from $\sigma'_{\rm PMT}$ (see table 1) to obtain estimates of the PMT transit time jitter, $\sigma_{\rm PMT}$. This procedure results in the estimates $\sigma_{\rm PMT}$ = 17.4 to 17.8 ps and 9.9 to 12.9 ps for PMT voltages of 3400 V and 3200 V, respectively. This is also the singlephoton time resolution one could hope for with ideal discriminators.

4.2 Estimate of Singlephoton Time Resolution in System with Time Walk Correction

The singlephoton time resolution obtainable in a system with time walk correction will not be quite as good as $\sigma_{\rm PMT}$, however. This is because the time walk correction can only correct for the dependence of the mean of the discriminator's time distribution on pulse amplitude. In addition to this dependence, the time assigned to a pulse by the discriminator also has a random error, which results in a non-zero standard deviation for each time distribution at constant pulse amplitude. Even though the magnitude of this standard deviation may

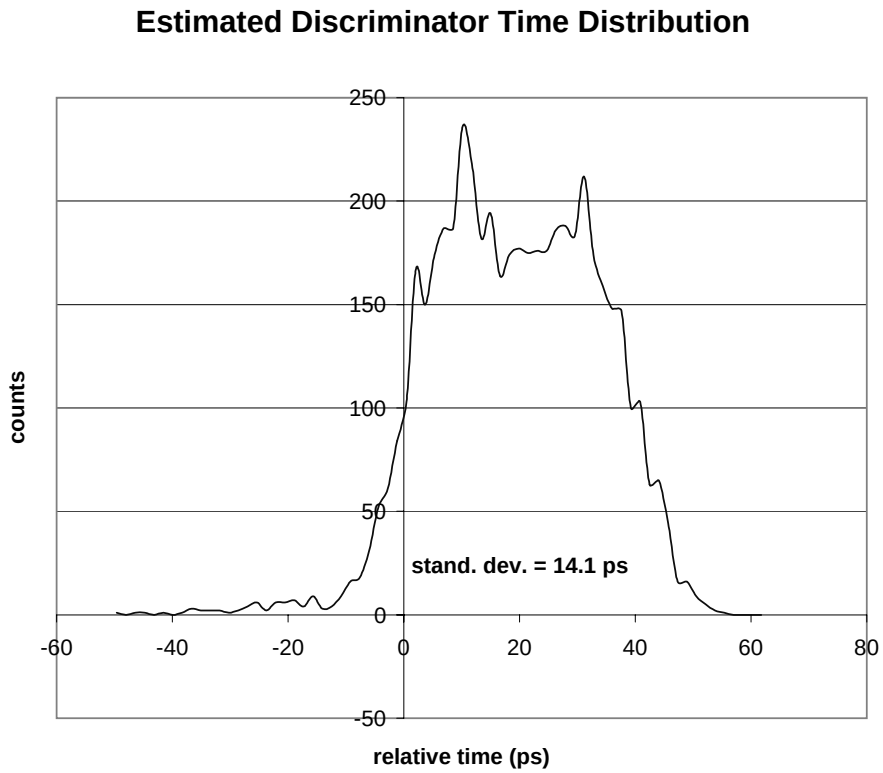

Figure 9: Time distribution of discriminator predicted by Monte Carlo simulation, based on the PMT singlephoton-gain distribution at 3400 V (fig.7) and the time walk distribution given in fig.5.

be dependant on pulse amplitude, it is still a random error that does not correlate with the amplitude, and thus cannot be corrected for.

In order to estimate the improvement expected from time walk correction, we repeated the Monte Carlo simulation as discussed above, but set the standard deviation of each (amplitude dependant) discriminator time distribution to zero. This resulted in discriminator time distributions with standard deviations $\sigma_{\rm disc} = 12.1$ ps and $\sigma_{\rm PMT} = 8.61$ ps for PMT voltages of 3400 V and 3200 V, respectively. Subtracting these numbers in quadrature from $\sigma'_{\rm PMT}$, we estimate the single photon time resolution in a system with time walk correction to be $\sigma_t = 18.9$ ps and 14.4 ps at 3400 and 3200 V, respectively.

4.3 Demonstration of Time Walk Correction

We can use the same Monte Carlo simulation to obtain a perhaps more explicit demonstration of the technique for time walk correction discussed above. We again simulate 5000 events, based on the pulseheight distributions measured for the PMT at 3400 V. We then generate two sets of data which represent timing data before and after discriminator time walk correction. The uncorrected data is generated as before, by generating a time shift for each pulse by drawing a number from a standard distribution with mean and standard

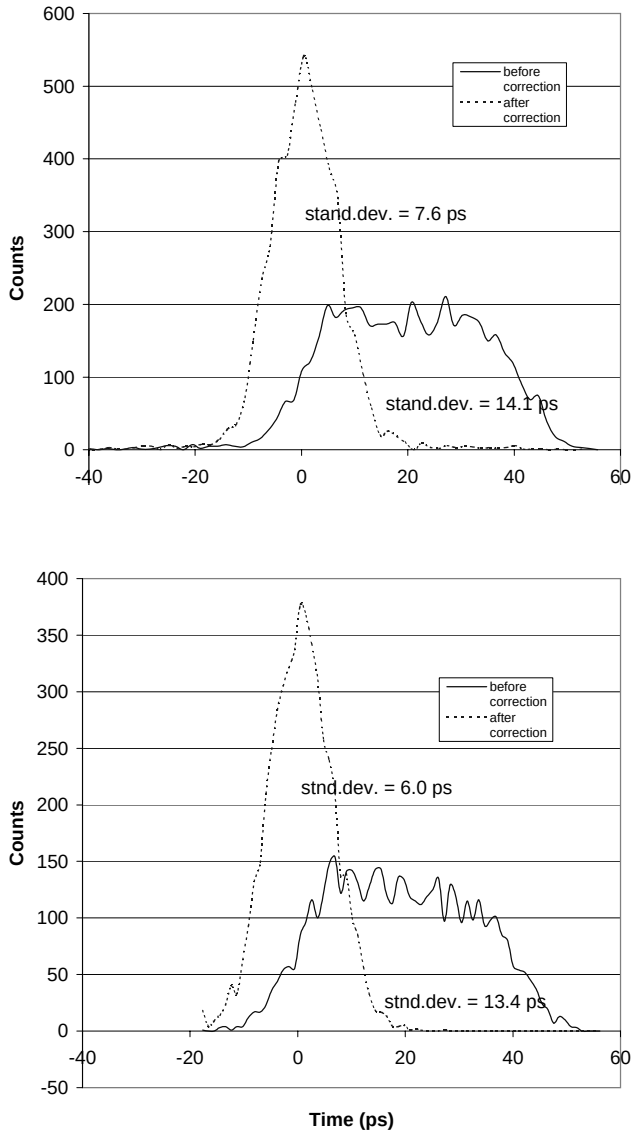

Figure 10: Estimation of improved discriminator timing through correction based on pulse amplitude, as discussed in text. The simulation resulting in the upper figure assumes a random timing error of 20 ps rms for pulses with amplitude below 150 mV. For the lower figure this number is 8 ps. Both cases for PMT voltage of 3400 V.

deviation appropriate for the amplitude of the respective pulse. For each pulse, we store the pulse amplitude and the generated time shift. This collection of time shifts represents our discriminator time distribution before time walk correction.

To simulate the time walk correction, we generate an additional data set from the uncorrected data. For each pulse, we look up the mean of the discriminator time distribution appropriate for the amplitude of the respective pulse, and subtract this from the uncorrected time shift. The collection of corrected time shifts make up the discriminator time distribution

after time walk correction. Figure 10 shows the resultant discriminator time distributions before and after correction for a PMT voltage of 3400 V. Because of the ill-characterized behavior of our system for low amplitude pulses, we ran two versions of the simulation, as discussed in the text of fig. 10. Note that the standard deviation of the corrected distributions agree well with what we would have expected from our predictions in section 4.2, that the systematic component of the discriminator time distribution (which is the component that can be corrected for) has an rms spread of 12.1 ps.

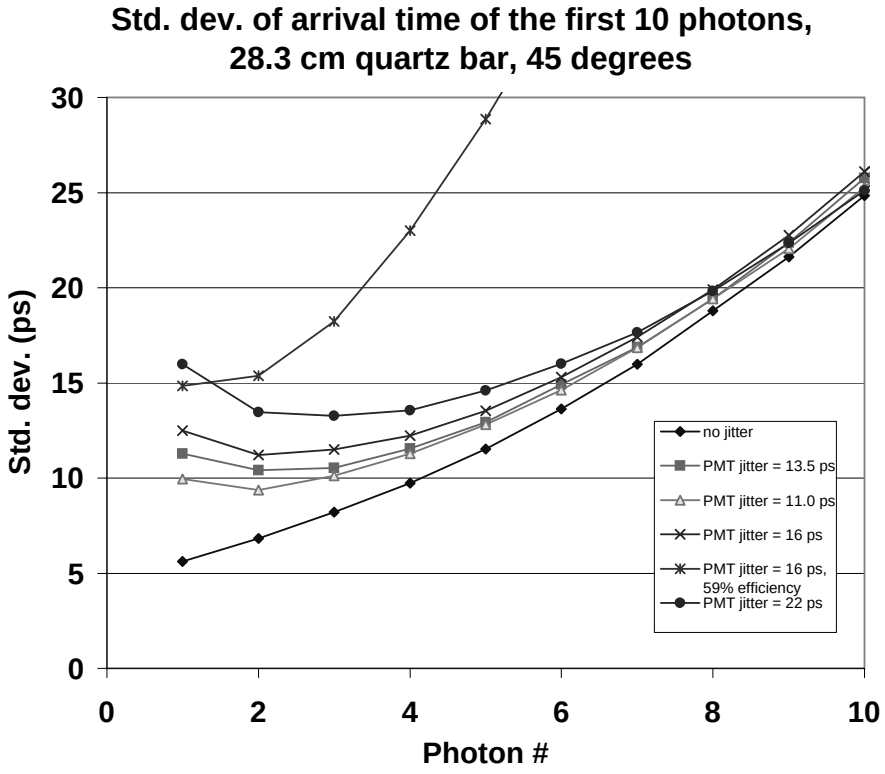

Figure 11: Predicted time resolution for Čerenkov photons from 165-MeV/c muons, for various singlephoton time resolutions (=PMT jitter in figure).

5 Discussion

The lowest transit-time spread measured for the Hamamatsu R3809U MCP-PMT, s/n ct100, was $\sigma t_{\mathrm{PMT}} \approx 16$ ps for a supply voltage of 3100 Volt. However, the pulse-height distributions for 3200 and 3400 Volt (see fig. 7) (as well as additional distributions which we have not included here) indicate that this result was most likely a tradeoff against photon-efficiency. Using (2), we obtain that for a supply voltage of 3200 Volts, the gain at the peak of the pulse-height distribution corresponds to a signal of 140 mV at the discriminator input. For a distribution measured at 3000 V, the peak had dropped below the discriminator voltage (-25 mV), which implies that the singlephoton detection efficiency drops dramatically as

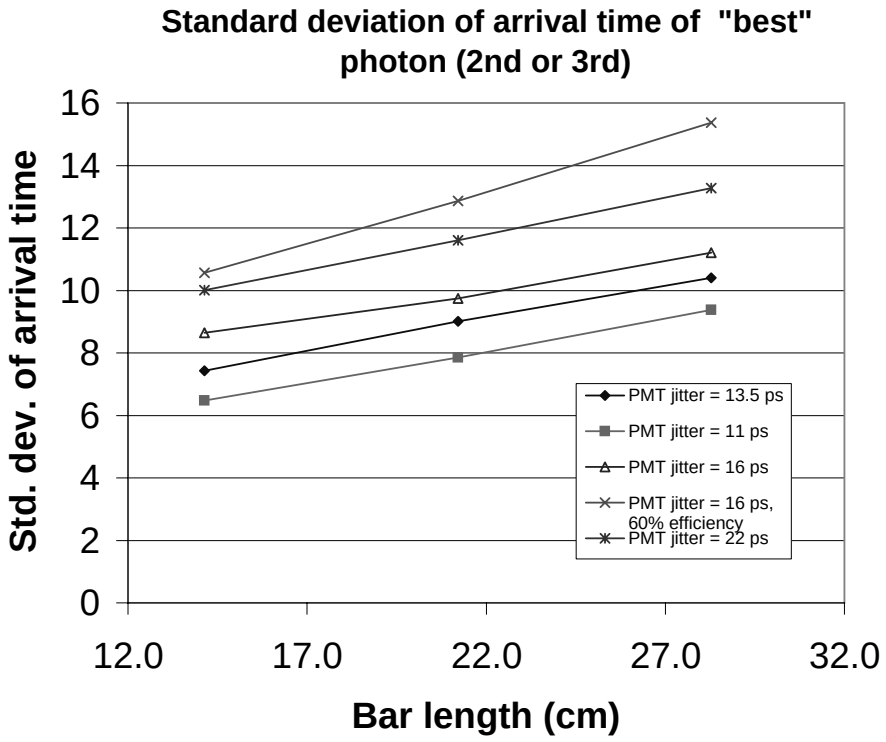

Figure 12: Predicted time resolution for Čerenkov photons from 165-MeV/c muons, for various singlephoton time resolutions (=PMT jitter in figure).

the high-voltage is decreased, since a substantial fraction of the PMT-pulses would have an amplitude to small to make it past the discriminator even at the lowest discriminator threshold, -25 mV.

This is confirmed by measurements of the pulse-rate versus PMT voltage (not included here). These measurements show that for a PMT voltage of 3400 Volts (maximum voltage stated by the manufacturer for the specific PMT), we detect 73000 pulses per second, while the rate falls of continously upon decreasing the PMT voltage. For instance, at 3000 V, the rate has dropped to 26000, which corresponds to only 35% of the maximum efficiency.

In a timing device where the signal consists of multiple photons (due to a charged particle's Čerenkov radiation), the time resolution will be affected by the lowered singlephoton efficiency. There is no simple and correct way to incorporate this effect into our simulation of a Cherenkov based timing device [4]. In this simulation, we simulated a constant threshold discriminator by "nth photon" timing, where the discriminator was triggered after the first n photons from a given pulse had arrived. There is an implicit assumption here that we can actually detect a single photon with constant probability. Instead, we find ourselves in a situation where the (amplified) PMT-output voltage due to a singlephoton pulse varies, and may not be high enough to trigger the discriminator. Within our approximation of nth photon timing, we can estimate the consequences for multi-photon pulses by simply disregarding a certain fraction of the arriving photons detected by the PMT in our simulation. For instance, at a PMT voltage of 3100 V, the single photon efficiency was measured to be

about 59%. To estimate the overall timing performance of a timing device at this PMT voltage, we therefore had the simulation disregard each photon detected by the PMT with a probability of 0.41. The results of this (perhaps overly naive) procedure indicate that the lowered single-photon efficiency lowers the overall time resolution drastically, see fig. 11 and fig.12. (The best time resolution predicted for any of the ordered photons is believed to be a good estimator for the overall time resolution of the timing device, see [4]).

The best strategy therefore seems to be to go to higher PMT voltages where the singlephoton detection efficiency is higher. Table 1 shows that this leads to a decreased single photon time resolution, which is partially explained by increased time jitter in the discriminator (see section 4). Some of the jitter in the discriminator can be corrected for by using pulse amplitude information to correct for the detection time. We predict that we could obtain a singlephoton time resolution σ_t of 18.9 ps at high photon detection efficiencies. Simulation results predict that this would enable us to time 165-MeV/c muons over a beam of 10-cm radius to $\sigma_t \approx 12.5$ps (see fig. 11). This assumes a timing device with 28 cm quartz bars. Since the time resolution depends strongly on the quartz bar length, we predict time resolution better than 10 ps if we could construct a device with bars shorter than about 18 cm (see fig.12).

6 Conclusion

We have measured the singlephoton time resolution of the Hamamatsu R3809U MCP-PMT (*including* jitter of detection electronics) to vary from $\sigma'_{\rm PMT} = 16$ps to 22 ps for PMT voltages from 3100 to 3400 V. Further measurements indicate that the best value of 16 ps measured at 3100 V was a trade off against singlephoton detection efficiency. A Monte Carlo simulation suggest that a substantial amount of the time jitter was due to the discriminator, so that the time resolution of the PMT itself can be estimated to be $\sigma_{\rm PMT} = 9.9$ to 17.8 ps, for supply voltages from 3200 to 3400 V.

A simulation based on "nth photon timing" [4] incorporating the above results, suggests that a timing device based on ultrafast PMT's viewing Čerenkov radiation from quartz bars will achieve time resolution on the order of 9 to 13 ps. These results include the predicted improvement from a system where the arrival time and amplitude of each PMT-pulse is stored and used to correct for discriminator time walk in software.

These results are encouraging, and we are currently preparing for measurements of singlephoton time resolution with a system incorporating time walk correction.

7 References

[1] C.M. Ankenbrandt *et al.*, *Ionization Cooling Research and Development Program for a High Luminosity Muon Collider*, (April 15, 1998);
http://www.fnal.gov/projects/muon_collider/cool/proposal/proposal.ps

[2] C. Lu *et al.*, *A Detector Scenario for the Muon Cooling Experiment*, Princeton/$\mu\mu$/97-8 (May 15, 1998);
http://puhep1.princeton.edu/mumu/mumu-97-8.ps

[3] A. Bross, Fermilab National Laboratory, private communication

[4] S.E. Vahsen and K.T. McDonald, *Precision timing via Čerenkov Radiation*, Princeton/$\mu\mu$/98-11 (July 25 1998);
http://puphep1.princeton.edu/mumu/timing.pdf

[5] *Technical Data: Ultrafast MCP-PMT R3809U*, Hamamatsu (Aug. 1992);
http://puhep1.princeton.edu/mumu/MCP-1.gif

[6] B. Gompf *et al.*, *Resolving Sonoluminescence Pulse Width with Time-Correlated Single Photon Counting*, Phys. Rev. Lett. **79**, 1405 (1997).

[7] Robert A. Hiller, Seth J. Putterman, and Keith R. Weninger, *Time-resolved Spectra of Sonoluminescence*, Phys. Rev. Lett. **80**, 1090 (1998).

[8] Michael J. Moran and Daren Sweider, *Measurements of Sonoluminescence Temporal Pulse Shape*, Phys. Rev. Lett. **80**, 4987 (1998).